Indian Journal of Pure & Applied Physics
Vol. 59, May 2021, pp. 391-397

Evolution of Superconducting Properties of Coexistent Bi-2212 and Bi-2223 phases in BSCCO

Gayathri V[a,b], A T Sathyanarayana[a,b], E P Amaladass[a,b], K Vinod[a,b], T Geetha Kumary[a], R Pandian[a,b] & Awadhesh Mani[a,b]*

[a]Materials Science Group, Indira Gandhi Centre for Atomic Research, Kalpakkam 603 102, Tamil Nadu, India.
[b]Homi Bhabha National Institute, Indira Gandhi Centre for Atomic Research, Kalpakkam 603 102, Tamil Nadu, India.

Received 24 August 2020; accepted 24 March 2021

The evolution of superconducting properties of BSCCO superconductors, inadvertently hosting the two superconducting phases Bi-2212 and Bi-2223 have been investigated in pristine and Pb doped BSCCO. The superconducting transition temperature T_C of Bi-2212 phase monotonically increases with increasing Bi-2223 phase fraction. On the other hand Bi-2223 phase exhibits depression in T_C for its lower phase fractions (<24%) but attains its bulk value as Bi-2223 phase fraction is increased to 30%. This behavior has been rationalized by invoking the interplay of proximity effects between the two coexisting phases and establishment of Bi-2223 superconducting percolation path. In addition to aiding the formation of BSCCO with higher Bi-2223 phase fraction, the Pb substitution also leads to an enhancement of critical current density by the creation of pinning centres.

Keywords: BSCCO, High temperature superconductivity, Proximity effect, Critical current density

1 Introduction

High temperature superconductors (HTSCs) have been a topic of perpetual interest because of their considerably high superconducting transition temperature (T_C), intricate nature of superconductivity and potential technological applications. Cuprate superconductors, accounting for the lion's share of the HTSCs, have layered structures where the phenomenon of superconductivity is observed in the Cu-O_2 plane with the spacer layers acting as charge carrier reservoirs[1-3]. Among the family of cuprate superconductors, Y-based HTSCs have been extensively studied. Bi-based superconductor BSCCO, being the first HTSC which did not contain a rare earth element, is another class of cuprate HTSC discovered in 1988 by Maeda *et al.*[1] with the general formula $Bi_2Sr_2Ca_{n-1}Cu_nO_{2n+4}$ where, n is the number of Cu-O_2 planes. Superconducting properties are found to be enhanced with an increase in the number of Cu-O_2 planes and n = 1, 2, and 3 correspond to Bi-2201, Bi-2212, and Bi-2223 phases respectively[3], with the corresponding superconducting transition temperature, T_C's of 20 K, 85 K, and 110 K. However, obtaining the phase pure Bi-2223 had remained extremely challenging task because of the complex reaction mechanism involved in the synthesis process and the intergrowth of the other phases[4] like Bi-2201 and 2212. Several strategies[5-12] have been employed in the attempt to get an enhanced superconducting property by increasing the phase fraction of Bi-2223 like addition of Pb[13,14], annealing the sample for prolonged duration near its melting temperature[4,9], controlling oxygen partial pressure during sintering[10] *etc*. Among these, Pb substitution in BSCCO has emerged as a promising strategy which not only aids in the enhancement of the superconducting critical temperature by stabilizing the Bi-2223 phase[15] but also increases the critical current density by acting as pinning centres[6].

The inadvertent presence of Bi-2212 phase along with Bi-2223 in the BSCCO samples provide a natural composite system in which two superconducting phases one with lower T_C residing in proximity with the other phase having higher T_C. In this scenario, it is interesting to investigate the evolution of the superconductivity in this composite system as a function of their phase fractions. With this objective, we have synthesized pristine and Pb-substituted BSCCO through solid state reaction route culminating in different phase fractions of Bi-2212 and Bi-2223 phases and performed detailed investigations on their superconducting properties. The evolutions of superconductivity of Bi-2212 and Bi-2223 phases in

*Corresponding Author (E-mail:mani@igcar.gov.in)

these systems have been qualitatively rationalized within the realm of proximity effect. The effect of Pb substitution on the enhancement of J_C, a property relevant from application point of view, is also investigated.

2 Materials and Methods

Polycrystalline samples of BSCCO and Pb-substituted BSCCO [B(Pb)SCCO] with starting composition $Bi_2Sr_2Ca_2Cu_3O_{10}$ and $Bi_{1.75}Pb_{0.25}Sr_2Ca_2Cu_3O_{10}$ respectively were prepared by solid state reaction route. High purity precursors (oxides and carbonates) were preheated to remove the moisture and then the stoichiometric amounts were weighed and ground to obtain a homogeneous mixture. The mixture was then calcined at 840 °C for 24 hrs at a slow heating and cooling rate of 2.7 °C/min. The calcined powder was then ground well, pelletized and sintered at 840 °C for 24 hr. It was then quenched in liquid nitrogen to arrest the state of the sample with the requisite property as the temperature window of the formation of the Bi-2223 phase is very narrow (835-855 °C). This process of grinding, pelletizing, and sintering with subsequent quenching of the sample was repeated many times to get the final sample with the required properties. Several sets of BSCCO and B(Pb)SCCO samples were synthesized which yielded different phase fractions of Bi-2212 and Bi-2223 by repeating the annealing conditions. BSCCO(0), BSCCO(19) and BSCCO(24) samples were obtained after repeating the process of grinding, pelletizing and sintering of the sample with the starting composition $Bi_2Sr_2Ca_2Cu_3O_{10}$ once, thrice, and five times, respectively. B(Pb)SCCO(30) was obtained after repeating the process of grinding, pelletizing and sintering of the sample with the starting composition $Bi_{1.75}Pb_{0.25}Sr_2Ca_2Cu_3O_{10}$ thrice. The structural properties of the samples were studied by X-ray diffraction (XRD) characterization performed in Laboratory Powder Diffractometer (D500 STOE) using *Cu-*K_α radiation (1.54 Å) in the θ-2θ Bragg-Brentano geometry. Morphological and elemental analyses of the samples were carried out using scanning electron microscopy (SEM) combined with energy dispersive X-ray spectroscopy (EDS) incorporated with a Peltier-cooled silicon drift detector. Temperature dependent DC electrical resistivity measurements in the temperature range of 4.2 to 300 K were measured via four probe method in Van der Pauw configuration for both the samples in an in-house built dip-stick cryostat. Magnetization measurements were carried out using a SQUID Magnetometer in the temperature range of 3 to 300 K and the magnetic field range of 0 to 7 T. Magneto-transport studies of BSCCO and B(Pb)SCCO samples were performed by applying the magnetic field perpendicular to the sample in the temperature range of 4-120 K and upto a magnetic field value of 15 T.

3. Results

The representative XRD patterns of a BSCCO as well as a B(Pb)SCCO samples are shown in Fig. 1. The peak positions are indexed by comparing with ICDD data. The phase percentage of Bi-2223 phase in BSCCO and B(Pb)SCCO is calculated using Eq. 1, where, $I^{0\,0\,10}_{Bi-2223}$ and $I^{0\,0\,8}_{Bi-2212}$ are the intensities of *(0 0 10)* and *(0 0 8)* which are the two nearby peaks of Bi-2223 and Bi-2212 phases, respectively, that are very well discernible[16].

$$X_{Bi-2223}\% = \frac{I^{0\,0\,10}_{Bi-2223}}{0.88\, I^{0\,0\,8}_{Bi-2212} + I^{0\,0\,10}_{Bi-2223}} \times 100 \qquad \ldots (1)$$

Among several sets of BSCCO and B(Pb)SCCO samples synthesized, the samples with systematically increasing Bi-2223 phase fractions of 0 %, 19 %, 24 %, and 30 % , designated as BSCCO(0), BSCCO(19), BSCCO(24), and B(Pb)SCCO(30), respectively, have been chosen for further studies. The crystal structures of both the phases present in these samples are found to be body centred tetragonal with the space group *I4/mmm*. The lattice parameters of Bi-2212 phase in BSCCO(24) are found to be a=3.81± 0.01 Å and c= 30.74± 0.01 Å, and that of the Bi-2223 phase are found to be a=5.39± 0.01 Å and c= 37.20± 0.01 Å. The a-lattice parameters for both the phases in

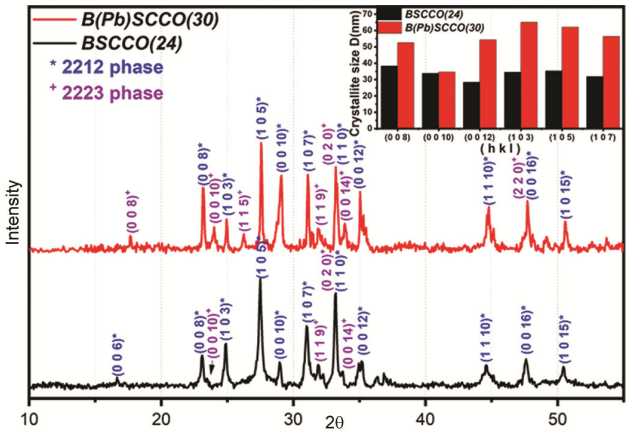

Fig. 1 — XRD patterns of BSCCO(24) and B(Pb)SCCO(30). Inset shows the variation of the crystallite sizes of the Bi-2212 phase with Pb substitution.

BSCCO(24) and B(Pb)SCCO(30) samples are found to be the same. However, the *c*-lattice parameters are found to decrease by 0.20 Å in B(Pb)SCCO(30) sample. The average crystallite size of Bi-2212 phase in BSCCO(24) and B(Pb)SCCO(30) extracted using Scherrer formula are found to be ~30±5 nm and ~50±5 nm, respectively. The EDS measurements confirmed the presence of all the constituent elements of these samples without any impurity. The compositions of the respective samples extracted from the EDS data are found to be $Bi_{2.28}Sr_{1.89}Ca_{1.48}Cu_{2.52}O_{10.82}$ and $Bi_{1.82}Pb_{0.22}Sr_{1.74}Ca_{1.55}Cu_{2.63}O_{11.53}$ with an error of ~2-5 %. The Sr/Ca ratio is determined for BSCCO(24) and B(Pb)SCCO(30) samples from their calculated composition. The Sr/Ca ratio for BSCCO(24) and B(Pb)SCCO(30) is found to be 1.28 and 1.12, respectively. A lower Sr/Ca ratio implies higher Bi-2223 phase fraction as Bi-2223 phase has twice the number of Ca atoms in comparison to Bi-2212 phase[17,18]. Hence the results from EDS measurement also supports the fact that Pb aids in the enhancement of Bi-2223 phase fraction in BSCCO.

Variation of temperature dependent electrical resistivity $\rho(T)$ of BSCCO(0), BSCCO(19), BSCCO(24), and B(Pb)SCCO(30) are shown in the Figs. 2(a-d)

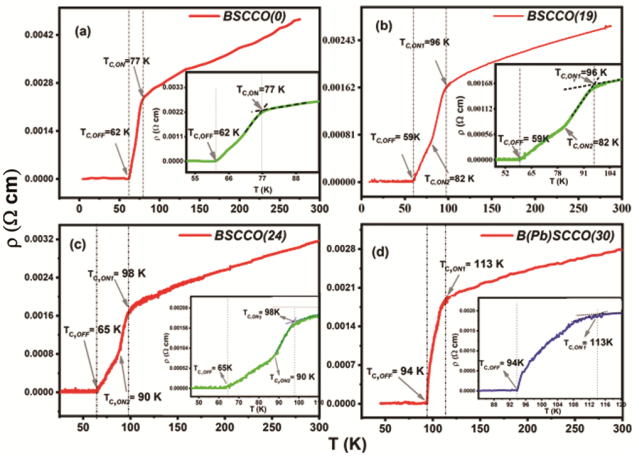

Fig. 2 — Electrical resistivity as a function of temperature (a)-(c) of BSCCO containing 0%, 19%, and 24% of Bi-2223 phase respectively and (d) B(Pb)SCCO with 30% of Bi-2223 phase. Inset in each graph highlights the superconducting transition region.

respectively. The onset superconducting transition temperature ($T_{C,ON}$) is obtained from the intersecting point of two tangents drawn around the region where $\rho(T)$ drops precipitously and the offset ($T_{C,OFF}$) is taken at temperature of occurrence of zero resistivity. $T_{C,ON1}$ corresponds to the superconducting transition onset of Bi-2223 phase and $T_{C,ON2}$ corresponds to that of Bi-2212 phase. ΔT_C represents the width of the superconducting transition. The values of $T_{C,ON1}$, $T_{C,ON2}$, $T_{C,OFF}$ and ΔT_C of all the samples, BSCCO(0), BSCCO(19), BSCCO(24), and B(Pb)SCCO(30) are tabulated in Table 1. Figure 2(a) represents the $\rho(T)$ curve of BSCCO(0). A single superconducting transition corresponding to Bi-2212 phase with a $T_{C,ON2}$ of 77 K and $T_{C,OFF}$ of 62 K is observed in this sample. The absence of $T_{C,ON1}$ hints to the absence of Bi-2223 phase. The $\rho(T)$ of BSCCO(19) is shown in Fig. 2(b). A double transition emanating from Bi-2212 and Bi-2223 superconducting phases are observed with $T_{C,ON1}$ at 96 K and $T_{C,ON2}$ at 82 K in this sample. The increase in ΔT_C from 15 K in BSCCO(0) to 37 K in BSCCO(19) arises on account of the presence of both phases in the latter. In BSCCO(24) sample, the $T_{C,ON1}$ and $T_{C,ON2}$ are found to be at 98 and 90 K, respectively, as seen in Fig. 2(c). The $\rho(T)$ of B(Pb)SCCO(30) as depicted in Fig. 2(d) reveals a single transition with $T_{C,ON1}$ of about 113 K which corresponds to the onset of Bi-2223 phase.

In order to bring out the effect of magnetic field on superconducting behaviour of Bi-2212 and Bi-2223 phases coexisting in pristine and Pb substituted BSCCO samples, the temperature dependence of the normalized resistance *[R(T)/R(120K)]* in the magnetic field range of 0 to 15 T for representative samples, BSCCO(24) and B(Pb)SCCO(30), are presented in Fig. 3(a) and 3(b), respectively. From Figs. 3(a) and 3(b), it is evident that the superconducting transitions broaden with the application of magnetic field which is indicative of the energy dissipation by the movement of fluxoids[19]. The resistance caused by the flux flow in the thermally activated region is given by the Arrhenius relation[20] given by Eq. 2, where U_0 is

Table 1 — T_C onset and offset of BSCCO and B(Pb)SCCO as obtained from the ρ(T) measurement.

Sample	$T_{C,ON1}$ (K) *(2223)*	$T_{C,ON2}$ (K) *(2212)*	$T_{C,OFF}$ (K)	ΔT_C (K)
BSCCO (0)	-	77	62	15
BSCCO (19)	96	82	59	37
BSCCO (24)	98	90	65	33
B(Pb)SCCO (30)	113	-	94	19

the activation energy, R_0 is the normal state resistance taken at 120 K and k_B is the Boltzmann constant.

$$R = R_0 \exp(-U_0/k_B T) \quad \ldots (2)$$

Figures 4(a-b) depicts $\ln(R/R_0)$ vs T^{-1} plots for different applied magnetic fields for BSCCO(24) and B(Pb)SCCO(30), respectively. Pinning activation energy (U_0) corresponding to Bi-2212 phase for all the samples have been extracted from the linear portion of $\ln(R/R_0)$ vs T^{-1} plots in low temperature regime below $T_{C,ON2}$. The values of U_0 at a field of ~0.002 T is found to be 256, 187, 99, and 1630 meV for BSCCO(0), BSCCO(19), BSCCO(24), and B(Pb)SCCO(30), respectively. The systematic

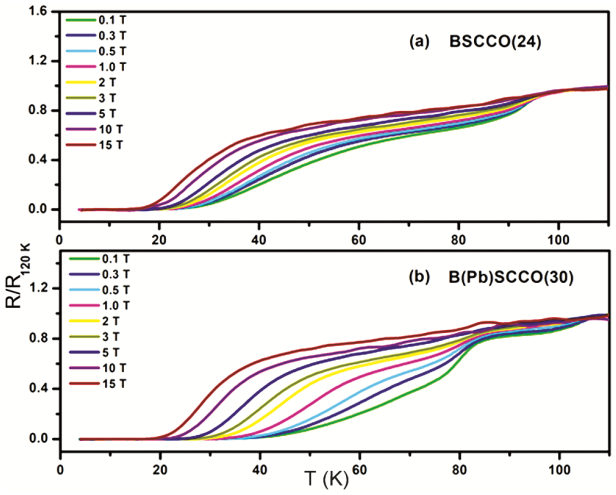

Fig. 3 — Temperature dependence of the normalized resistance in the magnetic field range of 0 to 15 T for (a) BSCCO(24) and (b) B(Pb)SCCO(30) bulk samples.

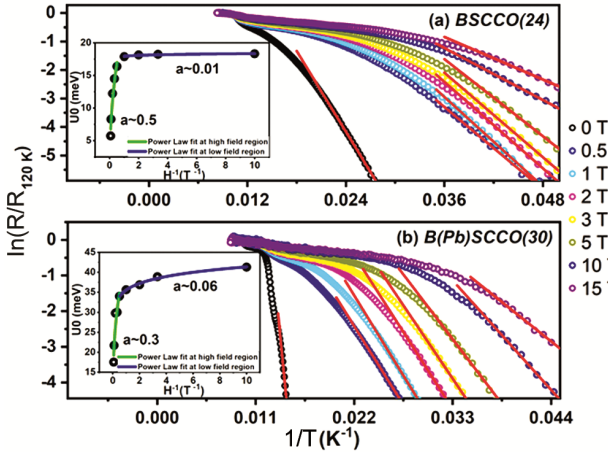

Fig. 4 — Arrhenius plots of R(T) for different applied magnetic fields for (a) BSCCO(24) and (b) B(Pb)SCCO(30) samples. Red lines represent the linear fit to extract U_o. Inset in each graph shows the power law dependence of U_o on H^{-1}.

decrease of U_0 in BSCCO samples may arise due to decrease in phase fraction of Bi-2212. The sudden increase in U_0 for B(Pb)SCCO(30) is attributed to enhancement in pinning centre caused by Pb substitution. The variation of U_0 with respect to the applied magnetic field (H) for Bi-2212 of BSCCO(24) and B(Pb)SCCO(30) is shown in the insets of Figs. 4(a-b), respectively. The field dependent behaviour of U_0 is further analyzed by performing a power law fitting to $U_0 \sim H^{-\alpha}$ as shown in the insets of Figs. 4(a-b). Here fitting parameter α implies the characteristic topological arrangement of the fluxoids. It is noteworthy to see that U_0 *vs* H fits to different values of α for low field ($H \leq 2T$) and high field ($H > 2T$) regimes. The values of α is found to be 0.01 and 0.06 in low field (LF) regime for BSCCO(24) and B(Pb)SCCO(30), respectively. In high field (HF) regime, on the other hand, the values of α increase to 0.5 and 0.3 for BSCCO(24) and B(Pb)SCCO(30), respectively. The value of α reflects the dimensionality of the vortex lattice; α = 0.3-0.5 corresponds to two dimensional arrangement of vortices[21]. This means that the arrangements of vortices appears to be two dimensional in HF regimes in these samples and is almost independent of field in the low field regime. Similar change over vortices behaviour from LF to HF regimes has been seen earlier[19].

Temperature dependent magnetization measurements were performed at various magnetic fields ranging from 0 to 7 T. Figures 5(a-b) show a representative zero field cooling (ZFC) and a field cooling (FC) curve for BSCCO(24) and B(Pb)SCCO(30), respectively, at an applied magnetic field of 0.01 T. The ZFC and FC curves clearly revealed the superconducting

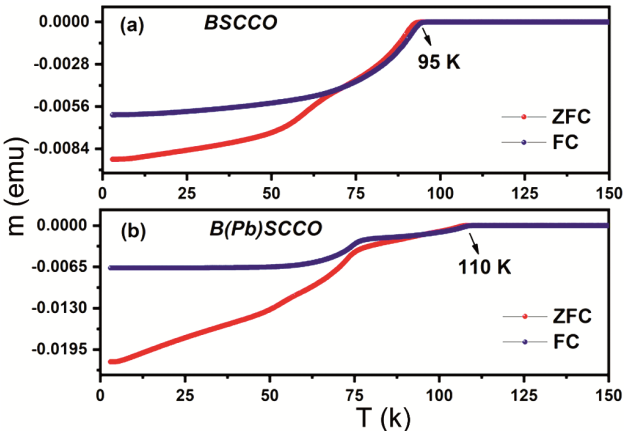

Fig. 5 — ZFC and FC magnetization (m) curves for (a) BSCCO(24) and (b) B(Pb)SCCO(30) at 0.01 T applied magnetic field portraying the T_C onsets.

transition onset at 95 and 110 K for BSCCO(24) and B(Pb)SCCO(30), respectively, which is located at a 3 K lower value than those obtained from ρ(T) measurements. A two step superconducting transition emanating from the presence of the two phases is evident from the magnetization curves. In order to investigate the evolution of critical current density (J_C), magnetic field dependent magnetization (M-H) measurements were performed at various temperatures for both the samples. A representative graph showing the M-H curve at T=3 K is shown in the inset of Fig. 6(a) from which J_C is calculated using Bean's model equation[22,23] given by Eq. 3, where, ΔM is the width of the magnetization loop at a certain magnetic field, and a and b are the breadth and length of the sample, respectively.

$$J_C=20\Delta M/a(1-(a/3b)) \quad \ldots (3)$$

Figures 6(a-b) shows the variation of J_C as a function of magnetic field at 3 K and as a function of temperature at 0.25 T, respectively. It is seen from these figures that B(Pb)SCCO(30) exhibits considerably higher values of J_C than that of BSCCO(24). The enhancement in J_C in B(Pb) SCCO(30) is consistent with the considerable increase observed in pinning potential U_0 in this sample. The pinning force density (F_P) for both the samples are calculated[24] using the Eq. 4.

$$F_P=\mu o\, J_C \times H \quad \ldots (4)$$

A representative plot of F_P of BSCCO(24) as function of field at various fixed temperatures is shown in Fig. 7. The inset in Fig. 7 compares field dependent F_P of BSCCO(24) and B(Pb)SCCO(30) at 3 K which complies with the fact that the Pb acts as a pinning centre, thereby preventing the motion of the vortex lines and hence resulting in higher $J_C(T,H)$ values[25].

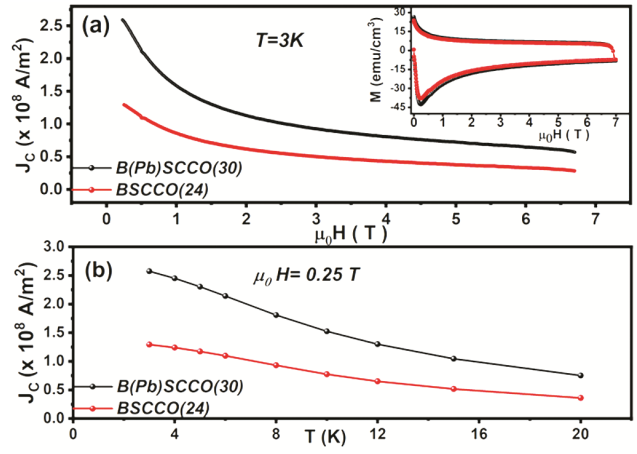

Fig. 6 — (a) The magnetic field dependent critical current density (J_C vs H) at 3 K and (b) the temperature dependent critical current density (J_C vs T) at 0.25 T for BSCCO(24) and B(Pb)SCCO(30). Inset in (a) shows a representative M-H curve at 3K used to deduce J_C.

4 Discussion

In what follows, we try to understand qualitatively the evolution of superconductivity in BSCCO and B(Pb)SCCO systems, comprising of Bi-2212 and Bi-2223 phases coexisting in proximity to each other, with the help of schematic diagram shown in Figs. 8(a-d). This explanation involves the effect of two phenomena, first, electrical conduction path facilitating percolation of Cooper pairs and the second, proximity effect induced modifications in properties of two superconducting phases, *i.e.*, Bi-2212 and Bi-2223. In this schematic representation, four regimes based on the systematic increase of Bi-2223 phase fraction (F_{2223}) in overall matrix of Bi-2212 phase are envisaged. Fig. 8(a) represents the first regime in which Bi-2223 phase content is negligibly small ($F_{2223} \rightarrow 0$), *e.g.,* BSCCO(0) which contains primarily Bi-2212 phase and yield $T_{C,ONI}$ ~77K (Fig. 2 (a)) close to its reported bulk value[2] of 80±3K. In second regime which contains low Bi-2223 phase content ($F_{2223} < 20\%$), the system is akin to Fig. 8(b). Here grains of Bi-2223 phase are sparsely dispersed in matrix of Bi-2212 phase. The electrical conduction path involves interconnection of primarily Bi-2212 phase in series with Bi-2223 as shown in Fig. 8(b). When superconductivity sets in high T_C Bi-2223 phase, the Bi-2212 phase remains in normal metallic state. In this scenario, Cooper pairs from

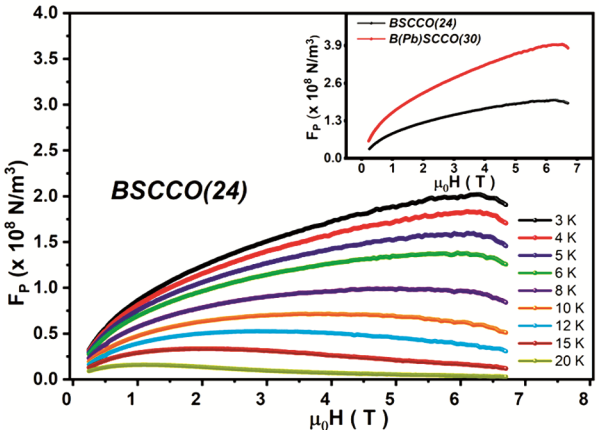

Fig. 7 — Magnetic field dependent inter-granular pinning force density (F_P) of BSCCO(24) at various temperatures. Inset illustrates the enhancement of F_P with Pb substitution.

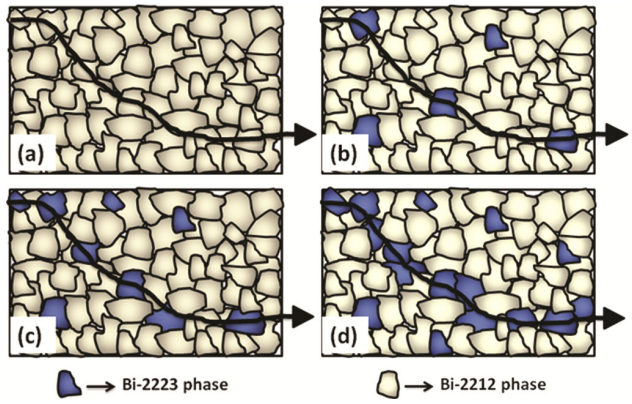

Fig. 8 — Schematic representation of evolution of Bi-2212 and Bi-2223 phases in (a) BSCCO(0), (b) (BSCCO(19), (c) BSCCO(24) and (d) B(Pb)SCCO(30).

Bi-2223 penetrate into adjacent Bi-2212 matrix. This results in decrease of T_C of Bi-2223 phase due to reduction in number density of cooper pairs from its bulk value. However, the number density of cooper pairs leaked from Bi-2223 grains into Bi-2212 matrix remains too small to cause appreciable enhancement in T_C of the latter above its bulk value. The sample BSCCO(19) represent this regime in which T_C ~ 96K of Bi-2223 phase is seen to be depressed from its bulk value (~110 K), while T_C of Bi-2212 phase changed only marginally to 82K (see Fig. 2(b)). Further increase of Bi-2223 phase content to intermediate value of F_{2223} ~ 25 %, representing third regime as shown in Fig. 8(c), leads to substantial enhancement in the number density of cooper pairs entering into Bi-2212, which boosts its superconductivity, giving rise to an increase in T_C of Bi-2212 phase above its bulk value. Simultaneously, due to the leakage of cooper pairs, there is a decrease in T_C of Bi-2223 phase, though to a lesser extent as compared to the second regime represented by Fig. 8(b). The sample BSCCO(24) conforms to the third regime and displays $T_{C,ON2}$ at 90 K which is much above the T_C onset of Bi-2212 phase, while $T_{C,ON1}$ at 98 K corresponding to that of Bi-2223 phase. It should be mentioned that in the third regime, as the $T_{C,ON1}$ still remain smaller than the bulk value of Bi-2223 phase, it is speculated that the phase content F_{2223} is not sufficient to provide full percolation path connecting the Bi-2223 grains. Fig. 8(d) represents the fourth regime in which phase content goes up beyond F_{2223} ~ 30 % and a percolation path is establishes within Bi-2223 grains. Here, due to availability of percolation path, $T_{C,ON1}$ pertaining to Bi-2223 exhibits its bulk value[1-2] close to ~110±5K. The Pb substituted sample namely B(Pb)SCCO(30) complies with this regime which exhibits only $T_{C,ON1}$ of 113 K corresponding to Bi-2223 as seen from Fig. 2(d). It should be remarked that the critical phase concentration required to attain percolation threshold for emergence of 3D superconductivity in cuprates is reported[26] to be around 30% which is in accordance with our result.

5 Conclusion

The effects of Pb substitution and annealing conditions on the superconducting properties of two coexisting phases, namely Bi-2212 and Bi-2223, in the BSCCO superconductor have been studied. It is observed that T_C of Bi-2212 phase monotonically increases over its bulk value with increase of Bi-2223 phase fraction. On the other hand T_C of Bi-2223 phase, which was initially depressed for lower phase fractions, resumes its bulk value as Bi-2223 phase fraction reaches 30%. This behavior has been rationalized by invoking proximity effect and establishment of Bi-2223 superconducting percolation path. Superconducting critical current density is found to be enhanced in B(Pb)SCCO as Pb acts as a pinning centre, thereby preventing the motion of the vortices.

Acknowledgement:

Authors are thankful to members of XCGS, MSG for XRD measurements on the samples. One of the authors (GV) is thankful to Department of Atomic Energy, India for the funding provided for her research work. Authors acknowledge UGC-DAE-CSR, Kalpakkam Node, for the SQUID magnetization and Magneto-resistance facilities.

References

1 Maeda H, Tanaka Y, Fukutomi M & Asano T, *Jpn J Appl Phys,* 27 (1988) L209.
2 Kumar J, Ahluwalia P K, Kishan H & Awana V P S, *J Supercond Nov Magn,* 23 (2010) 493.
3 Shalaby M S, Hashem H M, Hammad T R, Wahab L A, Marzouk K H & Soltan S, *J Radiat Res Appl Sci,* 9 (2016) 345.
4 Vinu S, Sarun P M, Shabna R, Biju A, Guruswamy P & Syamaprasad U, *Solid State Sci,* 11 (2009) 1150.
5 Camargo-Martínez J A & Baquero R, *Physica C,* 22 (2016) 521.
6 Biju A, Guruswamy P & Syamaprasad U, *Physica C,* 466 (2007) 23.
7 Mohammed N H, Awad R, Abou-Aly A I, Ibrahim I H & Hassan M S, *Mater Sci Appl,* 3 (2012) 224.
8 Giannini E, Bellingeri E, Passerini R & Flükiger R, *Physica C,* 315 (1999) 185.
9 Pakdil M, Bekiroglu E, Oz M, Saritekin N K & Yildirim G, *J Alloys Compd,* 673 (2016) 205.

10 Holesinger T G, Bingert J F, Willis J O, Maroni V A, Fischer A K & K T Wu, *J Mater Res,* 12 (2011) 3046.
11 Tsutom Y, Yoshihiko S, Soichi O, Hirofumi I, Masahiro Y, Makio N, Ryoichi T & Kohei O, *Jpn J Appl Phys,* 28 (1989) L972.
12 Takahira S, Ichino Y & Yoshida Y, *Phys Procedia,* 65 (2015) 153.
13 Kumar J, Ahluwalia P K, Kishan H & Awana V P S, *J Supercond Nov Magn*, 23 (2010) 493.
14 Nhien S & Desgardin G, *Phys C Supercond*, 272 (1996) 309.
15 Takano M, Takada J, Oda K, Kitaguchi H, Miura Y, Ikeda Y, Tomii Y & Mazaki H, *Jpn J Appl Phys*, 27 (1988) L1041.
16 Hu Q Y, Liu H K & Dou S X, *Physica C,* 250 (1995) 7.
17 Rai D K, Sarkar A K, Wittberg T N & Kumar B, *J Appl Phys*, 66 (1989) 3950.
18 Majewski P, Costa F M, Silva R F & Vieira J M, *Supercond Sci Technol*, 10 (1997) 453.
19 Palstra T T M, Batlogg B, van Dover R B, Schneemeyer L F & Waszczak J V, *Phys Rev B,* 41 (1990) 6621.
20 Palstra T T M, Batlogg B, Schneemeyer L F & Waszczak J V, *Phys Rev Lett,* 61 (1988) 1662.
21 Jurelo A R, Andrade S, Jardim R F, Fonseca F C, Torikachvili M S, Lacerda A H & Ben-Dor L, *Physica C,* 454 (2007) 30.
22 Bean C P, *Phys Rev Lett,* 8 (1962) 250.
23 A Ruyter, C Simon, V Hardy, M Hervieu & A Maignan, *Physica C,* 225 (1994) 235.
24 Krabbes G, Fuchs G, Canders W R, May H & Palka R, *High temperature superconductor bulk materials Fundamentals - processing - properties control - application aspects* (Wiley-VCH, Germany), 2006.
25 Chong I, Hiroi Z, Izumi M, Shimoyama J, Nakayama Y, Kishio K, Terashima T, Bando Y & Takano M, *Science,* 276 (1997) 770.
26 Pelc D, Vučković M, Grbić M S, Požek M, Yu G, Sasagawa T, Greven M & Barišić N, *Nat Commun,* 9 (2018) 4327.